AIAA JOURNAL
Vol. 30, No. 2, February 1992

Sound Generation by a Stenosis in a Pipe

J. C. Hardin*
NASA Langley Research Center, Hampton, Virginia 23665
and
D. S. Pope†
Lockheed Engineering & Sciences Company, Hampton, Virginia 23665

This paper presents a computational aeroacoustics study of sound generated by low Mach number flow through a closure (stenosis) in a circular pipe. The time-dependent incompressible flowfield in the pipe is first computed utilizing a vorticity/stream function formulation. The known velocity field is then utilized to determine the incompressible fluctuating pressure in the pipe. This hydrodynamic pressure field is then used to compute a hydrodynamic density perturbation to the constant incompressible density through the equation of state. Knowledge of this complete hydrodynamic field is then employed as the source of the resulting sound radiation. This tripartite technique allows separation of the compressible fluctuations from the purely hydrodynamic fluctuations. Results of the analysis are compared with experimental measurements of sound radiated by such a flow.

Introduction

SOUND generation by flow in pipes and ducts is important in many areas of technological interest. For example, ducted fans and jet engine compressors generate noise of concern to the aircraft community, whereas sound generation by valves and area changes in pipes can be a problem in architectural and industrial applications. The latter phenomenon is also beneficial in medicine for diagnostic purposes. Finally, there is currently much interest in surrounding a jet by a shroud, which has advantages in terms of noise reduction.

The sound generation by a limited region of turbulence in an infinitely long, square pipe was considered by Davies and Ffowcs Williams[1] and relevant scaling laws were derived. Doak[2] analyzed the sound field produced by source distributions in a finite length duct of arbitrary cross section and showed the dependence of the sound field on the duct mode structure and the source distribution. More recently, Michalke[3] examined noise generation by turbulence in a circular pipe carrying a uniform mean flow and again developed scaling laws.

To demonstrate a capability to handle various duct acoustic phenomena, this paper presents a computational aeroacoustics study of sound generated by low Mach number flow through a closure (stenosis) in a circular pipe. The time-dependent incompressible flowfield in the pipe is first computed utilizing a vorticity/stream function formulation. This solution shows the flow from the stenosis to be very like that of a shrouded jet. The known velocity field is then used to determine the incompressible fluctuating pressure in the pipe. The wall pressure fluctuations produced by such a flow were investigated by Abdallah and Hwang.[4] This hydrodynamic pressure field is then utilized to compute a hydrodynamic density perturbation to the constant incompressible density through the equation of state. Knowledge of this complete hydrodynamic field is then employed as the source of the resulting sound radiation. This technique allows separation of the compressible fluctuations from the purely hydrodynamic fluctuations. Results of the analysis are finally compared with experimental measurements of sound radiated by such a flow.

Statement of Problem

Consider the axisymmetric geometry shown in Fig. 1. A circular pipe of diameter D contains a cylindrical stenosis of length $2l$ in which there is a cylindrical passage of radius r_0. The pipe carries a mean inflow velocity U_0. Conditions at inflow are assumed known while the exit is open to the ambient atmosphere. It is further assumed that the inflow velocity is low enough and the stenosis radius large enough that the Mach number $M = \bar{U}/c_0 \ll 1$ everywhere in the pipe. Here, $\bar{U}(z)$ is the mean flow velocity through any cross section of the pipe and c_0 is the ambient speed of sound.

The flow within the pipe must satisfy the equations[5]

$$\frac{\partial \rho}{\partial t} + \frac{\partial}{\partial x_i}(\rho u_i) = 0 \tag{1}$$

$$\frac{\partial}{\partial t}(\rho u_i) + \frac{\partial}{\partial x_j}(\rho u_i u_j + p_{ij}) = 0 \tag{2}$$

where ρ and u_i are the density and velocity components, respectively, and

$$p_{ij} = p\delta_{ij} - \mu\left[\frac{\partial u_i}{\partial x_j} + \frac{\partial u_j}{\partial x_i} - \frac{2}{3}\left(\frac{\partial u_k}{\partial x_k}\right)\delta_{ij}\right]$$

is the compressive stress tensor with p the pressure and μ the coefficient of viscosity. In addition, an equation of state

$$p = p(\rho, S) \tag{3}$$

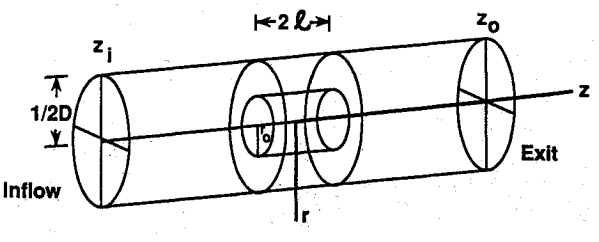

Fig. 1 Pipe geometry.

Received Aug. 24, 1990; presented as Paper 90-3919 at the AIAA 13th Aeroacoustics Conference, Tallahassee, FL, Oct. 22-24, 1990; revision received May 21, 1991; accepted for publication June 3, 1991.

*Senior Research Scientist.
†Principal Engineer.

relates the pressure, density, and entropy per unit mass S. This latter quantity must also satisfy the energy equation

$$T\frac{DS}{Dt} = c_p\frac{DT}{Dt} - \frac{\beta T}{\rho}\frac{Dp}{Dt} = \phi + 1/\rho\left(k\frac{\partial T}{\partial x_i}\right) \tag{4}$$

where T is the temperature; c_p, β, and k are the specific heat at constant pressure, coefficient of thermal expansion, and coefficient of thermal conductivity, respectively, of the fluid; and ϕ is the viscous dissipation function defined by Batchelor.[5]

Fluid Dynamics Calculation

A cylindrical coordinate system (r, θ, z) with corresponding velocity components (u_r, u_θ, u_z) is employed in the pipe, as shown in Fig. 1. The flowfield is assumed axisymmetric such that $u_\theta = \partial/\partial\theta = 0$. Although it would be preferable to employ a fully three-dimensional computational scheme, the cost of such calculations is still prohibitive. However, the axisymmetric assumption is made plausible by the flow visualization results of Cassanova and Giddens,[6] who found the low Reynolds number behavior of the flow distal to both sharp-edged and contoured stenoses to consist of axisymmetric vortex rings. This result is consistent with the fact that the flow from the stenosis is very like a shrouded jet, and it is known[7] that the preferred mode of a free jet at low Reynolds number is the axisymmetric vortex ring structure. Since the Mach number is low everywhere in the pipe, the incompressible approximation $\rho = \rho_0$ is also utilized in the flow calculation.

In such an axisymmetric flow, there is only one component of vorticity

$$\Omega = \frac{\partial u_r}{\partial z} - \frac{\partial u_z}{\partial r} \tag{5}$$

If one introduces the stream function Ψ such that

$$u_r = \frac{1}{r}\frac{\partial \Psi}{\partial z}, \qquad u_z = -\frac{1}{r}\frac{\partial \Psi}{\partial r}$$

then Eq. (1) is satisfied identically and Eqs. (2) and (5) may be used to obtain the governing equations

$$\nabla^2\Psi - \frac{2}{r}\frac{\partial \Psi}{\partial r} = r\Omega \tag{6}$$

$$\frac{\partial \Omega}{\partial t} + \frac{\partial}{\partial r}(u_r\Omega) + \frac{\partial}{\partial z}(u_z\Omega) = \nu\left[\nabla^2\Omega - \frac{\Omega}{r^2}\right] \tag{7}$$

where

$$\nabla^2 = \frac{\partial^2}{\partial r^2} + \frac{1}{r}\frac{\partial}{\partial r} + \frac{\partial^2}{\partial z^2}$$

and $\nu = \mu/\rho_o$.

The coupled set of partial differential equations (6) and (7) are numerically integrated in time from a nominal initial condition until steady state is reached. Steady state in this time-dependent flow is achieved when the amplitude of the resulting fluctuations no longer grows in time.

The initial conditions for the flow are taken to be

$$\Psi(r, z, 0) = \Omega(r, z, 0) = 0 \qquad z > z_i$$

while a parabolic inflow profile with mean velocity U_0 i.e.,

$$u_r(r, z_i, t) = 0$$

$$u_z(r, z_i, t) = 2U_0\left(1 - \frac{4r^2}{D^2}\right)$$

with corresponding stream function and vorticity

$$\Psi(r, z_i, t) = 2U_0\left(\frac{r^4}{D^2} - \frac{r^2}{2}\right)$$

$$\Omega(r, z_i, t) = \frac{16U_0 r}{D^2} \tag{8}$$

is specified for all time. At outflow, the extrapolation conditions

$$\frac{\partial \Psi}{\partial z}(r, z_0, t) = \frac{\partial \Omega(r, z_0, t)}{\partial z} = 0$$

are employed. Note that z_0 need not necessarily be the end of the pipe. On the walls, the no-slip condition $u_r = u_z = 0$ is utilized, which implies that

$$\Omega_{\text{wall}} = \frac{1}{r}\frac{\partial^2 \Psi}{\partial n^2}$$

where n is the outward normal to the wall, whereas on the centerline

$$\Psi(0, z, t) = \Omega(0, z, t) = 0$$

Finally, since the wall is a streamline, Eq. (8) yields

$$\Psi_{\text{wall}} = -\frac{u_0 D^2}{8}$$

Equations (6) and (7) are nondimensionalized using the mean flow velocity U_0 and the pipe diameter D, which amounts to replacing the kinematic viscosity ν in Eq. (7) by Re^{-1}, where

$$Re = \frac{U_0 D}{\nu}$$

is the Reynolds number of the flow. The nondimensionalized equations are then solved numerically on a uniform 59×66 grid covering the range $-1D < z < 1D$, as shown in Fig. 2. The grid spacing was chosen to make the wall vorticity computation compatible with the convergence criterion of the stream function iteration.

Since Eq. (7) is parabolic in time, its solution may be marched out in time from the given initial conditions using the conservative explicit-implicit predictor/corrector formulation developed by MacCormack.[8] At each time step, Eq. (6) is then solved iteratively using point-successive over-relaxation[9] to maintain the elliptic character of the incompressible flowfield.

Figure 3 presents the calculated stream function field at an instant of time after steady state has been achieved; whereas

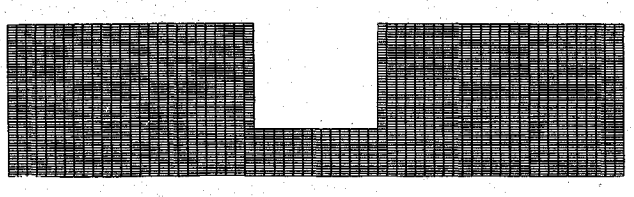

Fig. 2 59 × 66 computational grid.

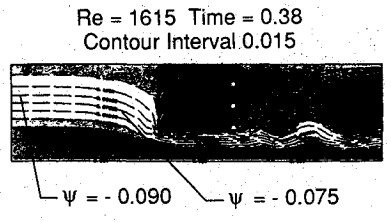

Fig. 3 Stream function at $t = 0.38$.

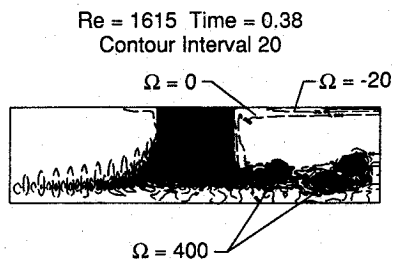

Fig. 4 Vorticity field at $t = 0.38$.

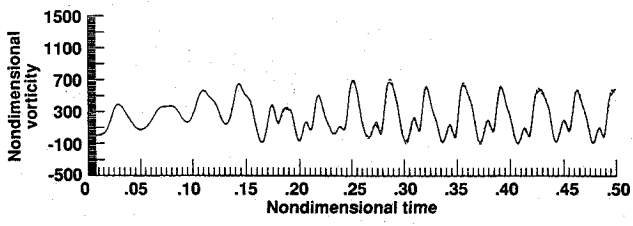

Fig. 5 Vorticity downstream of stenosis lip.

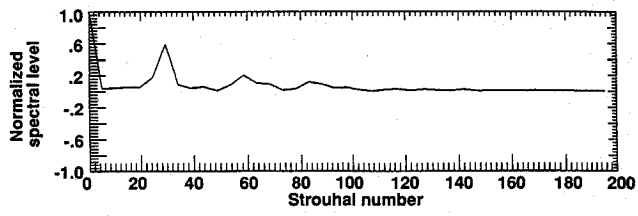

Fig. 6 Vorticity spectrum.

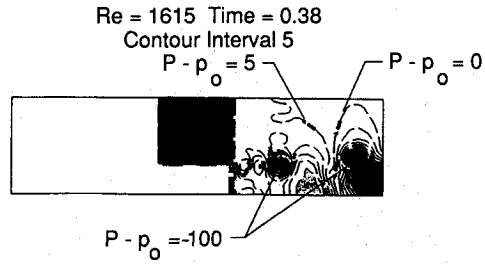

Fig. 7 Incompressible pressure field at $t = 0.38$.

Fig. 4 displays the corresponding vorticity field for a pipe Reynolds number of 1615 and a stenosis Reynolds number of 5135. At this Reynolds number, the flow in the pipe without stenosis would be laminar. Note that a jet-like flow develops downstream of the stenosis with sequential shedding of ring vortices. The vorticity seen upstream of the stenosis is steady and related to the mean flow gradients. Figure 5 presents normalized vorticity as a function of time at a point just downstream of the lip of the stenosis. Note that the vorticity fluctuations become nearly periodic after steady state is achieved. Figure 6 displays the spectrum of these vorticity fluctuations as a function of Strouhal number $St = fD/U_0$. Here, the fundamental fluctuation frequency and a couple of its harmonics may be observed. The peak Strouhal number is approximately 29 based on the pipe mean velocity and diameter. This translates into a Strouhal number of approximately 0.9, based on the stenosis mean velocity and diameter. Thus, if the flow from the stenosis can be considered as a jet, the Strouhal number of the shed vorticity is increased by a factor of approximately 3 over that ($St = 0.3$) ordinarily expected[7] for a free jet flow.

Incompressible Pressure Field Calculation

Once the incompressible velocity field has been computed, the corresponding incompressible pressure field may be obtained. Equation (2) may be manipulated to show that

$$\nabla^2 P = -\frac{\rho_0}{r}\left[\frac{\partial^2}{\partial r^2}(ru_r^2) + 2\frac{\partial^2}{\partial r\,\partial z}(ru_r u_z) + \frac{\partial^2}{\partial z^2}(ru_z^2)\right] = -s(r, z) \tag{9}$$

where $P(r, z, t)$ is the incompressible pressure field and the source term is known from the velocity field. In addition, the gradient boundary conditions $\partial P/\partial n$ on the boundary surfaces are known from Eq. (2). This equation may be readily solved via a Green's function,[10] i.e.,

$$P(r, z) = C + \int_V G(r,\theta,z,r',\theta',z')\, s(r',z')\, dV + \int_S G(r,\theta,z,r',\theta',z')\frac{\partial P}{\partial n}(r',z')\, dS \tag{10}$$

where $G(r,\theta,z,r',\theta',z')$ satisfies

$$\nabla^2 G = -(1/r)\delta(r - r')\delta(\theta - \theta')\delta(z - z') + (1/V)$$

in the volume V downstream of the stenosis ($l \le z \le z_0$) and $\partial G/\partial n = 0$ on the surrounding surface S. The constant C reflects the nonuniqueness of this Neumann problem and can be evaluated by a knowledge of the pressure at one point in the field.

The required Green's function may be readily obtained via standard techniques. Since the source terms in Eq. (10) are independent of θ', the integral of Eq. (10) over θ' may be eliminated by recording only

$$\int_0^{2\pi} G(r,\theta,z,r',\theta',z')\, d\theta' = -\frac{1}{R^2}\left[\frac{2L}{3} - |z-z'| - (z + z' - 2l) + \frac{[(z-l)^2 + (z'-l)^2]}{L}\right] - \frac{1}{R^2}\sum_{m=2}^{\infty}\frac{J_0(\gamma_m r)J_0(\gamma_m r')}{[J_0(\gamma_m R)]^2} \times \frac{\cosh\gamma_m(L - |z - z'|) + \cosh\gamma_m(L + 2l - z - z')}{\gamma_m \sinh\gamma_m L} \tag{11}$$

where $L = z_0 - l$, $R = D/2$, and the γ_m are the tabulated roots of $J_0'(\gamma_m R) = 0$.

Using Eq. (11) in Eq. (10), the incompressible pressure field $P(r,z)$ may be computed at each time step. The constant C was determined from a knowledge of the pressure at one point in the flow for experimental data to be discussed later. Figure 7 displays the computed pressure field corresponding to the stream function and vorticity fields shown in Figs. 3 and 4. Note the low pressures at the center of the concentrated vorticity clusters.

Hydrodynamic Density Field Calculation

The pressure field computed from Eq. (10) varies both in space and time. Thus, pressure changes

$$dp(r,z,t) = P(r,z,t) - p_o$$

where p_o is the ambient pressure, are taking place in the flow. Although these changes were computed under the assumption of constant density, no fluid is truly incompressible, and Eq. (3) implies that

$$dp = \left(\frac{\partial p}{\partial \rho}\right)_s d\rho + \left(\frac{\partial p}{\partial S}\right)_\rho dS = c^2\, d\rho + \left(\frac{\partial p}{\partial S}\right)_\rho dS \tag{12}$$

where the speed of sound in the medium is defined by

$$c = \left(\frac{\partial p}{\partial \rho}\right)_S^{1/2}$$

This relation shows that any pressure changes must be balanced by a combination of density changes and entropy changes, where the entropy changes further satisfy Eq. (4), i.e.,

$$T\frac{DS}{Dt} = \phi + \frac{1}{\rho}\frac{\partial}{\partial x_i}\left(k\frac{\partial T}{\partial x_i}\right)$$

However, Batchelor[5] notes that, in estimating the magnitude of pressure fluctuations, one loses little generality by assuming the flow to be isentropic, because the effects of viscosity and heat conduction are normally to modify the pressure distribution rather than to control the magnitude of the pressure variation. Thus, if one defines the time average pressure distribution

$$\bar{P}(r,z) = \lim_{T\to\infty}\frac{1}{T}\int_0^T P(r,z,t)\,dt$$

and pressure fluctuations

$$p_1(r,z,t) = P(r,z,t) - \bar{P}(r,z)$$

about this time average, one may assume the time-averaged pressure to be the result of dissipative mechanisms, whereas the fluctuations about the time average may be taken as isentropic.

Under this assumption, Eq. (12) shows that the incompressible pressure fluctuations $p_1(r,z,t)$ must be balanced by density fluctuations $\rho_1(r,z,t)$, i.e.,

$$p_1(r,z,t) = c^2\rho_1(r,z,t) \tag{13}$$

even in the incompressible flow. This seemingly contradictory result can be explained by noting that

$$\frac{\rho_1}{\rho_o} = M^2\frac{p_1}{\rho_o U_o^2}$$

Thus, at low Mach number, the density fluctuations may be safely neglected in computing the incompressible pressure field. However, these hydrodynamic density fluctuations that take place in the incompressible flow can be shown to be quite large in comparison to the acoustic density fluctuations. Equation (13) is utilized to compute the "correction" $\rho_1(r,z,t)$ to the incompressible density with, as usual for low Mach number, the sound speed c replaced by its ambient value c_o.

Calculation of Sound Field

Consider now the solution of the compressible flow governed by Eqs. (1-4). Let

$$u_i = U_i + u_i', \qquad p = P + p', \qquad \rho = \rho_o + \rho_1 + \rho' \tag{14}$$

where u_i' and p' are the fluctuations in the velocity components and pressure about their incompressible counterparts and ρ' is the fluctuation of the density about the corrected incompressible density $\rho_o + \rho_1$. The primed quantities are basically acoustic variables since the purely hydrodynamic fluctuations have been included in the corrected incompressible flow.

From Eqs. (1) and (2), Lighthill[11] derived the exact acoustic analogy

$$\frac{\partial^2\rho}{\partial t^2} - c_o^2\nabla^2\rho = \frac{\partial^2 T_{ij}}{\partial x_i\partial x_j} \tag{15}$$

where

$$T_{ij} = \rho u_i u_j + (p - c_o^2\rho)\delta_{ij} + \mu\left[-\frac{\partial u_i}{\partial x_j} - \frac{\partial u_j}{\partial x_i} + \frac{2}{3}\left(\frac{\partial u_k}{\partial x_k}\right)\delta_{ij}\right]$$

from which the sound generated by a fluid flow could be calculated if the source term T_{ij} were known. He also suggested that, at low Mach number, the approximation $T_{ij} \cong \rho_o U_i U_j$, where the U_i are the incompressible velocity components, would often be valid.

If Eqs. (14) are employed in Eq. (15) and the approximation $T_{ij} \cong (\rho_o + \rho_1)U_iU_j$ based on the corrected incompressible velocity field is employed, Eq. (15) becomes

$$\frac{\partial^2(\rho_1 + \rho')}{\partial t^2} - c_o^2\nabla^2(\rho_1 + \rho') = \frac{\partial^2}{\partial x_i\partial x_j}[(\rho_o + \rho_1)U_iU_j] \tag{16}$$

Thus, Lighthill's original approximation amounts to solving a wave equation for the sum $\rho_1 + \rho'$. This can only be appropriate in the far field since $\rho_1 \sim x^{-2}$ while $\rho' \sim x^{-1}$ where x is the source/observer distance. However, by Eqs. (9) and (13),

$$c_o^2\nabla^2\rho_1 = \nabla^2 P = -\rho_o\frac{\partial^2}{\partial x_i\partial x_j}(U_iU_j) \tag{17}$$

Thus, adding Eqs. (16) and (17) and rearranging,

$$\frac{\partial^2\rho'}{\partial t^2} - c_o^2\nabla^2\rho' = -\frac{\partial^2\rho_1}{\partial t^2} + \frac{\partial^2}{\partial x_i\partial x_j}(\rho_1U_iU_j) = S(r,z,t) \tag{18}$$

Equation (18) is used to calculate the sound field produced by the stenosis. It has the advantages over Eq. (16) that only the acoustic fluctuation is computed and that the source term is nonzero only where the hydrodynamic density perturbation is non-negligible.

Equation (18) is again solved via a Green's function technique. To simplify the problem, two assumptions are made: 1) reflections from the open end of the pipe are ignored, and 2) the effect of the stenosis on the sound field is partially ignored. The former assumption implies that oscillations at the resonant frequencies of the pipe will not appear in the analysis. Whereas these may be important to the total sound field produced by the pipe, one may view the pipe as a linear system that is forced by the flow though the stenosis. Since the main interest of this work is to determine this acoustic forcing function, the readily identified resonances of the pipe are ignored.

The latter assumption has several aspects. First, only sound sources downstream of the stenosis are considered. Clearly, this is the region where the most intense fluctuations are taking place. Further, the work of Agarwal,[12] who experimentally investigated turbulent pipe flow disturbed by an orifice plate, concluded that the flows upstream and downstream of the plate behaved as if they were acoustically independent. Thus, any sound generated upstream of the stenosis is assumed to be reflected by the stenosis. On the other hand, any reflection of the sound generated downstream by the stenosis is neglected. In fact, the sound field is calculated as if the stenosis were not there at all. This is done for analytical convenience and could be eliminated by doing more of the computations numerically. However, it is partially justified by the fact that, as will be seen later, only plane waves can propagate in the duct and thus the duct shape is not of critical importance.

It should be mentioned that although the Lighthill source term given in Eq. (15) is quadrupole in nature, the solution to

this equation when such sources are surrounded by a pipe shows that the quadrupole sources induce more efficient dipole-type sources on the pipe walls, just as they would on any nearby surface. This is the reason that the scaling studies[1,3] have always found a U_o^6 dependence of the sound power radiated from turbulence in a duct, characteristic of an acoustic dipole, rather than the U_o^8 dependence that would be expected from a quadrupole source. Thus, neglect of the stenosis in the acoustic solution merely replaces dipole sources on the stenosis surface by dipole sources on the pipe wall.

Under these assumptions, one may employ the Green's function solution to Eq. (18) developed by Goldstein[13] for an infinitely long cylindrical pipe. Ignoring viscous effects on the sound field such that $\partial\rho/\partial r = 0$ on $r = R$, Goldstein shows that the solution to Eq. (18) is

$$\rho'(r,z,t) = \int_{-T}^{T} d\tau \int_V S(r',z',t') \times G(r,\theta,z,t,r',\theta',z',t')r'\,dr'\,d\theta'\,dz' \tag{19}$$

where

$$\frac{\partial^2 G}{\partial t^2} - c_o^2 \nabla^2 G = \frac{c_0^2}{r}\delta(t-t')\delta(r-r')\delta(\theta-\theta')\delta(z-z')$$

such that $\partial G/\delta r = 0$ on $r = R$ and T is a large time. This Green's function is then obtained in terms of the modes of the pipe.

Green's function may be greatly simplified by noting that the cut-on frequency of the first nonplane mode is

$$f = 0.586(c_0/D)$$

or a Strouhal number of $St = 0.586/M$. At the Mach number of the experimental data ($M = 0.003$), this Strouhal number is well above those of interest, and thus, only the plane wave mode will propagate in the pipe. Therefore, if one is some distance downstream of the source region, all one will see is the propagating plane wave. In this case, the required Green's function is given approximately by

$$G(r,\theta,z,t,r',\theta',z',t') \simeq \frac{H[c_0(t-t') - |z-z'|]}{4\pi R^2 c_0} \tag{20}$$

where $H[\,]$ is the Heaviside function. Thus, the acoustic field becomes independent of the radial coordinate r and Eq. (19) yields

$$\rho'(z,t) \simeq \frac{1}{2R^2c_0}\int_{-T}^{T} dt' \int_l^{z_0} dz' \times H[c_0(t-t') - |z-z'|]\hat{S}(z',t') \tag{21}$$

where

$$\hat{S}(z',t') = \int_0^R r'\left[\frac{\partial^2}{\partial z'^2}(\rho_1 u_z^2) - \frac{\partial^2 \rho_1}{\partial t'^2}\right] dr'$$

Equation (21) may be further greatly simplified by integration by parts (for $z > z_0$) to yield

$$\rho'(z,t) \simeq \frac{-1}{2R^2c_0}\int_{t-\frac{z}{c_0}}^{t-\frac{(z-z_0)}{c_0}} dt' \int_l^{z_0} dz' \times \delta[c_0(t-t') - (z-z')]\tilde{S}(z',t') \tag{22}$$

where $\delta[\,]$ is the Dirac delta function and

$$\tilde{S}(z',t') = \int_0^R dr'\,r'\left(\frac{\partial(\rho_1 u_z^2)}{\partial z'} + c_0\frac{\partial \rho_1}{\partial t'}\right)$$

Equation (22) is used to produce the acoustic results of this study. Note that this computational technique does not assume the source to be compact.

Comparison with Experimental Data

The experimental data used in this research were obtained by Robert F. Coleman and Gary L. Schechter of the Eastern Virginia Medical School, Vocal Dynamics Laboratory as a part of a study of the use of noninvasive acoustic techniques to diagnose closures of the windpipe. The model consisted of a flexible tube of length 48 cm and inside diameter of 2.5 cm. Obstruction segments 1 cm thick were cast of the same rubber-like material with various size circular openings and could be positioned at various locations in the tube. These tests are very similar to those described by Gordon[14] at somewhat higher Reynolds numbers employing ring spoilers in a pipe.

An air source was provided by a SCUBA tank and associated regulator. The flow rate was measured by a venturi flow gauge, and provision for mean pressure measurements was provided at various distances along the pipe. Finally, the sound radiated by the stenosis was measured by a 1.25-cm (0.5-in.) microphone with noise cone at the exit of the pipe and aligned with the flow.

In an experimental configuration such as this, extraneous noise sources caused by interaction of the outflowing turbulence with the lip of the pipe and monopole noise generated by fluctuations in mass flow across the nozzle exit plane are theoretically possible. However, in a similar experiment, Gordon[15] found that neither the exit plane nor the turbulence flowing across it were of fundamental importance. Further, no evidence of monopole-like radiation was found for a well-regulated inlet flow. The dominant noise generating region was determined to be located near the spoiler rather than at the pipe exit.

In addition, unwanted sound produced by flow over the microphone is a possibility. However, the microphone noise cone is designed to eliminate such generation to much higher flow velocities than considered herein.

A typical result of this study is shown in Fig. 8, which is the spectrum of sound radiation from the pipe carrying air at a mean velocity of 95.4 cm/s (3.1 ft/s). At 8 cm from the exit of the pipe, a stenosis exists representing 90% closure of the pipe. The pipe Reynolds number is 1615, whereas the stenosis Reynolds number is 5135, the same values as were used in the computational study.

Measurements of the acoustic response of the pipe with stenosis in place were also made by exciting the pipe with a white noise source. The spectrum of the pipe response is shown in Fig. 9. The observed resonances agree reasonably well with the frequencies (1031, 3094, and 5157 Hz) predicted by the closed-open-end organ pipe analysis, i.e.,

$$f_n = \frac{(2n+1)}{4L_p} \qquad n = 0, 1, 2, \ldots$$

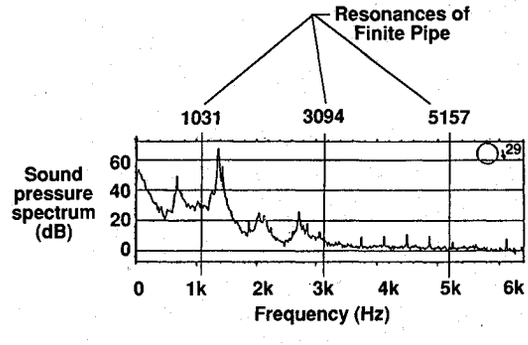

Fig. 8 Sound radiation by pipe stenosis.

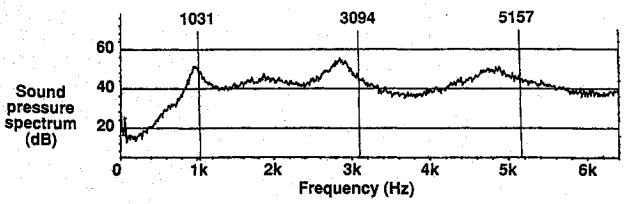

Fig. 9 Acoustic response of pipe with stenosis.

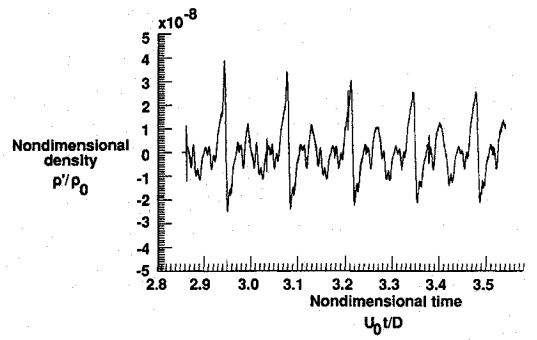

Fig. 10 Acoustic density fluctuations at observer position.

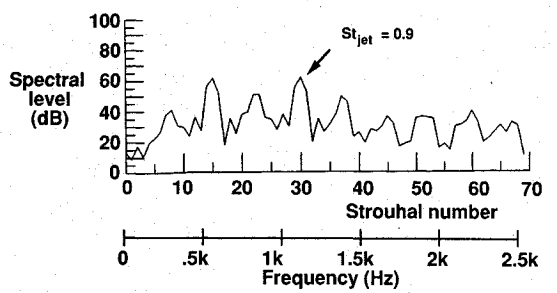

Fig. 11 Predicted acoustic spectrum.

where L_p is the length of the pipe. In comparing Fig. 8 with Fig. 9, it will be seen that the pipe resonances are not in evidence in the stenosis spectrum and, thus, the observed spectral levels must be primarily due to the forcing function provided by the jet-like flow from the stenosis.

The computational aeroacoustics analysis described earlier was applied for the precise geometry and flow conditions pertaining to the experimental measurements, except that the termination of the pipe was ignored. Figure 10 presents the calculated time history of acoustic density at an observer location $4D$ downstream of the stenosis. This position corresponds roughly to the microphone location in the experimental tests. Note that the time history is nearly periodic with a rapid oscillation occurring at equal intervals.

Figure 11 is the predicted acoustic spectrum estimated from the time history shown in Fig. 10 as a function of the Strouhal number, $St = fD/U_0$, of the pipe. Although the resolution and accuracy of this spectral estimate is limited by the short data length, note that the peak amplitude occurs near the Strouhal number of 30, corresponding to that seen in the vorticity fluctuations of Fig. 6, with a secondary peak near the Strouhal number of 15. Also shown in Fig. 11 are frequencies corresponding to the experimental measurement conditions. The highest spectral level at a Strouhal number of 30, which corresponds to a frequency of 1127 Hz, agrees reasonably well both in frequency and amplitude with the highest spectral level seen in the experimental data of Fig. 8. The next highest amplitude ($St = 15$) at the frequency 563 Hz agrees reasonably well in frequency but somewhat overpredicts the amplitude of the second highest peak in the data of Fig. 8 (neglecting the very low frequency background noise.)

Conclusions

A computational aeroacoustics study of sound generation by a stenosis in a cylindrical pipe has been carried out. The study used a tripartite technique, whereby the incompressible flow was calculated and used to determine a hydrodynamic correction to the constant incompressible density that was then used in the source term to calculate the resulting acoustic field. The calculated acoustic field was then compared with experimental data. Based on this study, the following conclusions may be drawn.

1) The tripartite technique is valid, at least at the low Mach and Reynolds numbers of the present study, in that it yields acoustic spectra that agree reasonably well both in amplitude and frequency with experimental data.

2) The flow downstream of the stenosis (90% closure) is very like that of a shrouded jet with peak fluctuations occurring at a Strouhal number near 0.90, based on the stenosis velocity and diameter. This is nearly three times the Strouhal number $St = 0.3$ expected for a free jet flow.

3) Assuming the characteristic Strouhal number to be reasonably invariant with stenosis contour, an estimate of the stenosis diameter and, hence, percent closure can be obtained for medical diagnostic purposes from a knowledge of the pipe diameter, mass flow rate, and peak frequency of sound radiation.

Acknowledgment

The authors wish to express their appreciation to Robert F. Coleman and Gary L. Schechter of the Eastern Virginia Medical School, Vocal Dynamics Laboratory for providing the experimental data.

References

[1]Davies, H. G., and Ffowcs Williams, J. E., "Aerodynamic Sound Generation in a Pipe," *Journal of Fluid Mechanics,* Vol. 32, Pt. 4, 1968, pp. 765–778.

[2]Doak, P. E., "Excitation, Transmission and Radiation of Sound from Source Distributions in Hard-Walled Ducts of Finite Length (I): The Effects of Duct Cross-Section Geometry and Source Distribution Space-Time Pattern," *Journal of Sound and Vibration,* Vol. 31, No. 1, 1973, pp. 1–72.

[3]Michalke, A., "On the Propagation of Sound Generated in a Pipe of Circular Cross-Section with Uniform Mean Flow," *Journal of Sound and Vibration,* Vol. 134, No. 2, 1989, pp. 203–234.

[4]Abdallah, S. A., and Hwang, N. H. C., "Arterial Stenosis Murmurs: An Analysis of Flow and Pressure Fields," *Journal of the Acoustical Society of America,* Vol. 83, No. 1, 1988, pp. 318–334.

[5]Batchelor, G. K., *An Introduction to Fluid Dynamics,* Cambridge Univ. Press, Cambridge, England, UK, 1967, Chaps. 1,3.

[6]Cassanova, R. A., and Giddens, D. P., "Disorder Distal to Modeled Stenoses in Steady and Pulsatic Flows," *Journal of Biomechanics,* Vol. 11, 1978, pp. 441–453.

[7]Crow, S. C., and Champagne, F. H., "Orderly Structure in Jet Turbulence," *Journal of Fluid Mechanics,* Vol. 48, Pt. 3, 1971, pp. 547–591.

[8]MacCormack, R. W., "A Numerical Method for Solving the Equations of Compressible Viscous Flow," AIAA Paper 81-0110, Jan. 1981.

[9]Hoffman, K. A., *Computational Fluid Dynamics for Engineers,* Engineering Education System, 1989.

[10]Roach, G. F., *Green's Functions,* 2nd ed., Cambridge Univ. Press, Cambridge, England, UK, 1982.

[11]Lighthill, M. J., "On Sound Generated Aerodynamically: 1. General Theory," *Proceedings of the Royal Society of London, Series A: Mathematical and Physical Sciences,* Vol. 211, 1952, pp. 564–587.

[12]Agarwal, N., "Generation and Propagation of Sound Waves in Disturbed Pipe Flow," AIAA Paper 90-0286, Jan. 1990.

[13]Goldstein, M. E., "Aeroacoustics," NASA SP-346, 1974.

[14]Gordon, C. G., "Spoiler-Generated Flow Noise. II. Results," *Journal of the Acoustical Society of America,* Vol. 45, No. 1, 1969, pp. 214–223.

[15]Gordon, C. G., "Spoiler-Generated Flow Noise. I. The Experiment," *Journal of the Acoustical Society of America,* Vol. 43, No. 5, 1968, pp. 1041–1048.